

Capacitive MEMS Accelerometer with Open-loop Switched-capacitor Readout Circuit

Michał Szermer, *Member, IEEE*, Piotr Amrozik, Piotr Zajac, Cezary Maj,
and Andrzej Napieralski, *Senior Member, IEEE*

Abstract—MEMS are one of the fastest developing branch in microelectronics. Many integrated sensors are widely used in smart devices i.e. smartphones, and specialized systems like medical equipment. In the paper we present the main parts of a system for measuring human movement which can be used in human balance disorder diagnosis. We describe our design of capacitive accelerometers and dedicated switched-capacitor readout circuit. Both will be manufactured as separate chips in different technological processes. The principle of operation, schematics and layouts of all parts of the system are presented. Preliminary simulations show that the proposed designs are applicable for the considered medical device.

Index Terms—MEMS, ASIC, accelerometer, integrated circuit, balance disorder.

I. INTRODUCTION

THE idea of measuring inertial forces is known from many years. Its importance is driven by the necessity of determining body movement. It is possible by using mechanical elements which are sensitive to velocity or acceleration. Mechanical measuring systems used before the era of microelectronics were very large. The breakthrough in microelectronic technology in the 1970s allowed manufacturing mechanical sensors in microscale. They are known as MEMS (Micro-Electro-Mechanical Systems) and have experienced rapid growth in recent years [3], [6], [7], [15], [16], [19], [23], [26], [31], [35], [36], [40], [41], [42], [10]. The first commercial inertial sensors fabricated in micromachining technology were accelerometers. The 50g accelerometer, which was used in airbag ignition devices, played the pioneering role. Since then MEMS inertial sensors started to be developed quickly [2], [17], [20], [22], [28], [30], [35], [36], [38], [39], [43], [53], [58], [59].

Meanwhile, more and more complex and sophisticated ASICs (Application Specific Integrated Circuit) were designed. The constant development of microtechnologies available for designers, the constant decrease of prototyping cost and the availability of manufacturing small number of chips in Multi-Project Wafer (MPW) services encourage researchers to design circuits containing both MEMS and ASICs.

In this paper we describe the first approach to the design of capacitive MEMS accelerometer with open-loop switched-

capacitor readout circuit which will be used for medical purposes: diagnosing elderly people with balance disorders. This device should be small, low-power, with easy and fast wireless communication interface. It will help medical staff to provide a quick response in case of health problems [3], [6], [15], [23], [26], [27], [46].

II. MEMS DESIGN

A. Accelerometers overview

There are many proposed solutions for MEMS accelerometers [2], [17], [20], [22], [45], [56], [57], [58], [60]. The most popular are capacitive accelerometers [30], [31], [39], [59]. The operation principle of these sensors is based on measuring the capacitance change when inertial forces appear. The sensor is built from two plates which form a capacitor. One plate is movable and is called a proof mass, while the second one is fixed to the substrate. When the acceleration appears the proof mass changes its position with respect to the fixed part, which causes the capacitance change.

The typical values of capacitance in such sensors are very small (in the order of pF) and the capacitance change is even lower. To improve the sensor parameters like sensitivity comb-drive structures are usually used. The typical comb-drive accelerometer consists of two combs with many fingers. One comb is connected to the proof mass, and the second one is fixed to the substrate. Each pair of fingers (movable and fixed) form a capacitor. The use of many fingers allows the increase of the total capacitance. The initial capacitance of such sensor is described by the following formula [30], [52]:

$$C_0 = \varepsilon \frac{ns}{d} \quad (1)$$

where S is the area of one finger, n is the number of fingers in one comb, d is the distance between fingers and ε is the electrical permittivity. The capacitance change due to applied acceleration is as follows:

$$\Delta C = C_x - C_0 = \varepsilon \frac{ns}{d-x} - C_0 \quad (2)$$

where x is the distance change between fingers.

M. Szermer, C. Maj, P. Zajac, P. Amrozik and A. Napieralski are with the Department of Microelectronics and Computer Science, Lodz University of Technology, Łódź, Poland (email: szermer@dmcs.pl).

Results presented in the paper are supported by the project STRATEGMED 2/266299/19NCBR/2016 funded by The National Centre for Research and Development in Poland.

The behaviour of MEMS inertial sensors (like accelerometers) is described by second order differential equation [37], [39]:

$$ma_x = m \frac{d^2x}{dt^2} + b \frac{dx}{dt} + kx \quad (3)$$

where m is the mass of the movable part, b is the damping coefficient and k is the suspension stiffness.

According to the equation (3) the analytical solution of the acceleration may be calculated if all parameters are known. This approach allows estimating the general sensor performance quickly. In case of complex sensor shapes it is difficult to calculate the parameters of equation (3). Therefore, other methods are employed and the most popular one is the Finite Element Method (FEM). There are also mixed methods which use both analytical and numerical methods. This approach is employed for example in MEMS+ by Coventor® [13] which is used in our design.

There are many methods for measuring the acceleration with such sensors. It was decided to use differential method: a differential pair of capacitors is formed in such a way that the first capacitance increases, the second decreases and the difference between them is measured. As a result, the capacitance change occurs in both capacitors and the difference in their capacitances is proportional to the acceleration (for very small displacements). The principle of this method is presented in Fig. 1.

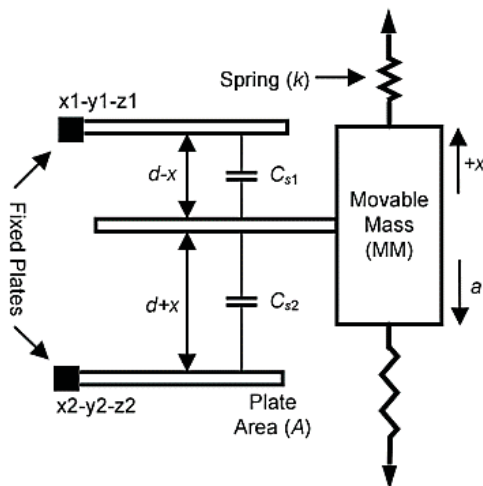


Fig. 1. The principle of measuring acceleration in a capacitive accelerometer [44].

B. One-axis capacitive accelerometer design

During our research various accelerometer structures were tested. First, an one-axis accelerometer were designed with H-shaped proof mass. This allows placing many fingers connected to the proof mass. Other fingers are attached to the frame, which is fixed to the substrate. The schematic and layout view of the baseline accelerometer is shown in Fig. 2. and Fig. 3. Its dimensions are $864\text{ }\mu\text{m} \times 624\text{ }\mu\text{m}$. Next, the scaling factor (SF)

was introduced in order to resize the baseline structure. All accelerometer dimensions in X and Y plane were parametrized using the SF except for the distance between fingers and finger thickness. Thus we obtained the possibility of changing the accelerometer properties just by modifying SF in order to find the optimal value of the sensor sensitivity [24], [32], [47], [52]. Due to technology constraints, the SF value was limited to the range from 1.0 to 2.0. After preliminary analysis it was decided to design three structures (SF=1.0, SF=1.5, SF=2.0) in the first MEMS prototype.

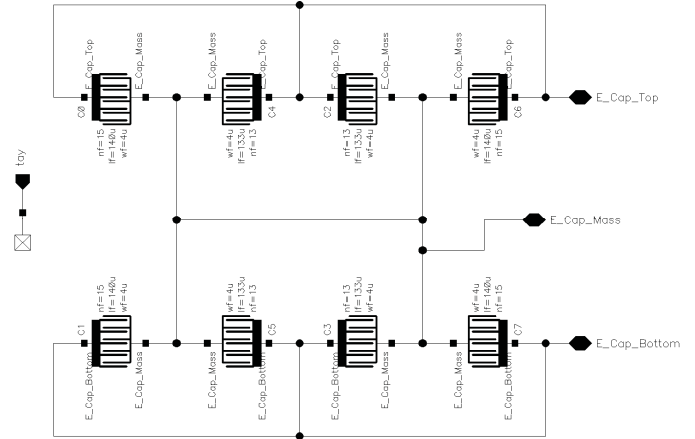


Fig. 2. Accelerometer schematic view.

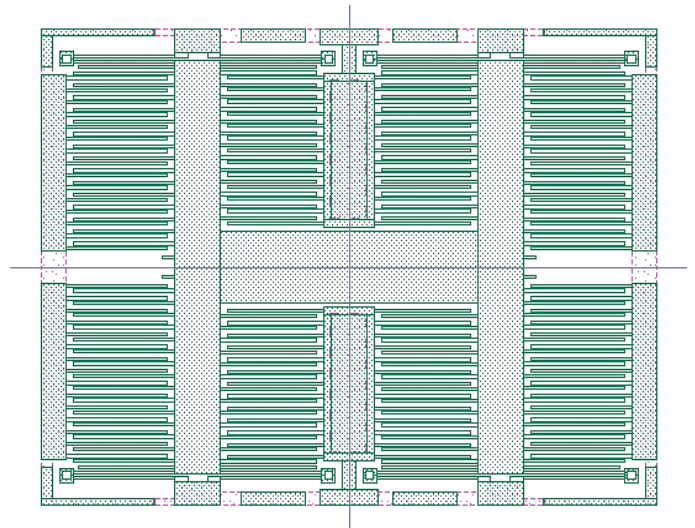


Fig. 3. Accelerometer layout view.

C. Simulation results

All simulations were performed by coupling MEMS+ software with Cadence Spectre. First, the MEMS+ 3D accelerometer model was exported to Cadence environment. Then, the simulations of this model were run in Spectre. During simulations the operation of the accelerometer was computed on-the-fly by MEMS+. As the input, the linear acceleration change from 0 to $8g$ was set. Next, the following simulation

types were performed: *modal*, *DC* and *DC sweep* analysis. The first eigenfrequencies of the tested accelerometers are shown in Table I.

TABLE I.
LIST OF THE FIRST EIGENFREQUENCIES OF THE ACCELEROMETER
FOR DIFFERENT VALUES OF THE SCALE FACTOR

Scale Factor (SF)	Frequency [Hz]
1.0	16 800.2
1.5	6 043.1
2.0	2 998.2

The capacitance change of these accelerometers were also calculated. The simulation results for the SF=1.0 and SF=1.5 and the acceleration change from 0 to 8g are presented in Fig. 4. The capacitance in an equilibrium state and the sensitivity calculated for the selected sensors are shown in Table II.

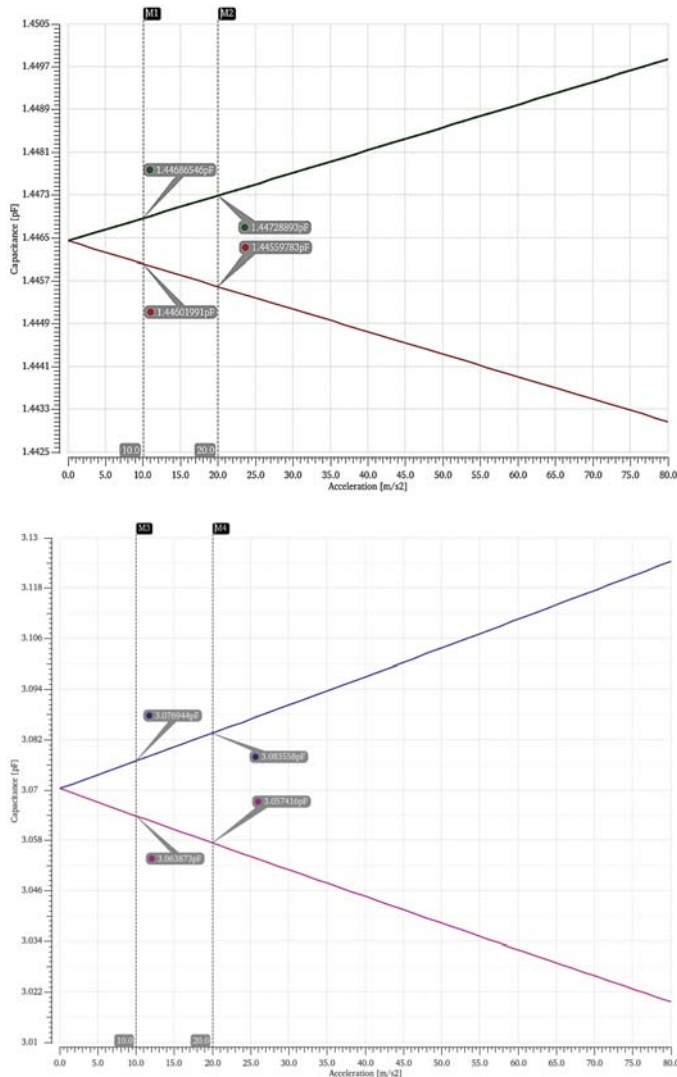


Fig. 4. Simulation results of a DC sweep analysis with SF=1.0 (top) and SF=1.5 (bottom).

TABLE II.
LIST OF THE CAPACITANCES AND SENSITIVITIES OF THE ACCELEROMETER
FOR DIFFERENT VALUES OF THE SCALE FACTOR

Scale Factor (SF)	Sensor Capacitance [pF]	Sensitivity [fF/g]
1.0	1.446	0.888
1.5	3.152	8.390
2.0	5.729	64.275

The initial capacitance is the lowest and also the sensitivity is the lowest for the SF=1.0. Both the sensor capacitance and the sensitivity increase with SF. This is beneficial from the designer's point of view, however it is worth pointing out that for the SF=2.0, nonlinearities in the output were visible. The non-linearity of the sensor output is undesirable because it causes the readout circuit to be more complex. Therefore, the structure with SF=2.0 was discarded from further analysis.

D. Layout of the accelerometers

Two structures were tested and the first prototype containing two accelerometers were prepared (see Fig.5). This design is ready for sending to the silicon foundry, however, it will be probably modified by adding the one additional structure. It is in the test phase and will operate in Z-axis. Accelerometers shown in Fig. 5. have the SF=1.0 and SF=1.5. In the Fig.5 the symmetry according to the Y-axis is visible (two identical structures on the right and left). This was required by the chosen technology and is necessary to reduce stress, which appears during cutting the dies.

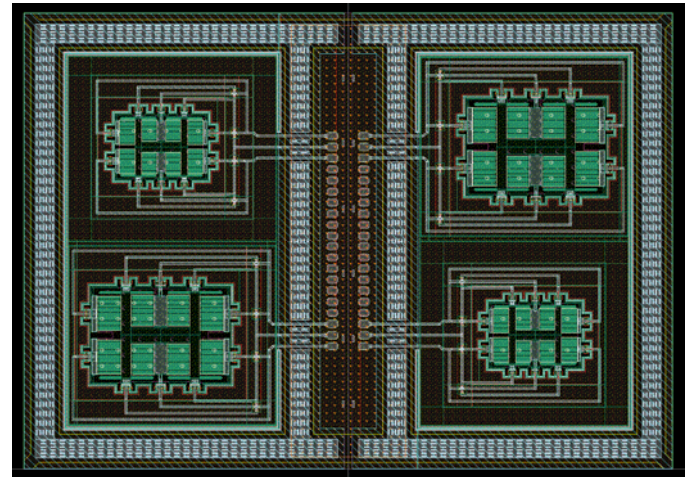


Fig. 5. The layout view of two accelerometers.

III. ASIC DESIGN

A. Overview

Described accelerometer (MEMS) requires dedicated ReadOut Integrated Circuit (ROIC) [1], [5], [14], [18], [21], [33], [49], [50], [53], [55], [58] in order to make their output signal useful. This circuit is designed as separate ASIC in a different process technology. Generally, it consist of three modules: MEMS Signal Readout (MSR), Radio-chip Interface

(RI), Reference Signal (RS) (see Fig. 6). The main task of the MSR module is to process signals from MEMS sensors, to convert them to digital domain using analog-to-digital converter (ADC). We chose 10-bit successive-approximation ADC. Next, the ADC output is delivered to the RI module, whose main task is to transmit received data via SPI to the low-power Bluetooth device [9], [34]. The third block is the RS module necessary for delivering the reference signals to all circuits in ASIC.

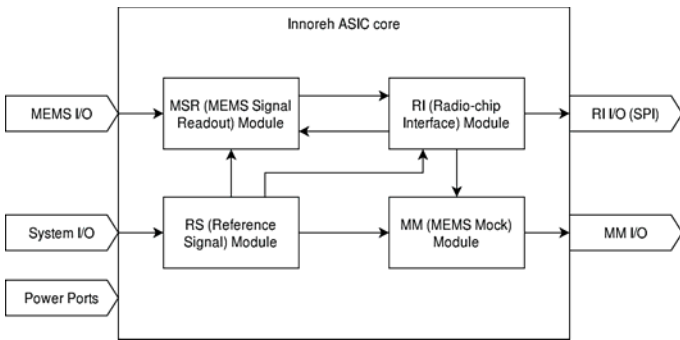


Fig. 6. ASIC block diagram.

B. Design and simulations

The ASIC is a mixed-signal circuit [4], [8], [25], [48], [54]. The most important part of the ASIC is the MSR, which converts very small capacitance change from the sensors to the voltage. Therefore, this module, whose layout had to be designed in full-custom approach, is the most demanding part of the ASIC. MSR architecture employs switched-capacitor techniques [4], [8], [33]. One of the advantages of this solution with respect to continuous-time circuits [4], [8] is the elimination of the need for large resistors, which reduced the layout size. The block diagram of the readout circuit used in the ASIC is shown in Fig. 7. Pseudo-differential circuit was designed [21], [44], [53]. The principle of operation is to deliver modulating signal to the proof mass of the accelerometer (middle node) and read outputs from the top and bottom plates of the capacitors (top and bottom node). Two clock signals $clk1$ and $clk2$ are used in the chip with the frequency of 400 kHz. Such high frequency is necessary to avoid causing the electrostatic force on the MEMS accelerometer plates, as this frequency is far outside the bandwidth of the accelerometer. Each clock activates a different phase of the operation, namely charging phase (when $clk1$ is active) during which the MEMS capacitances are charged with known voltage and readout phase (when $clk2$ is active), when the charge from MEMS capacitances is converted to the voltage.

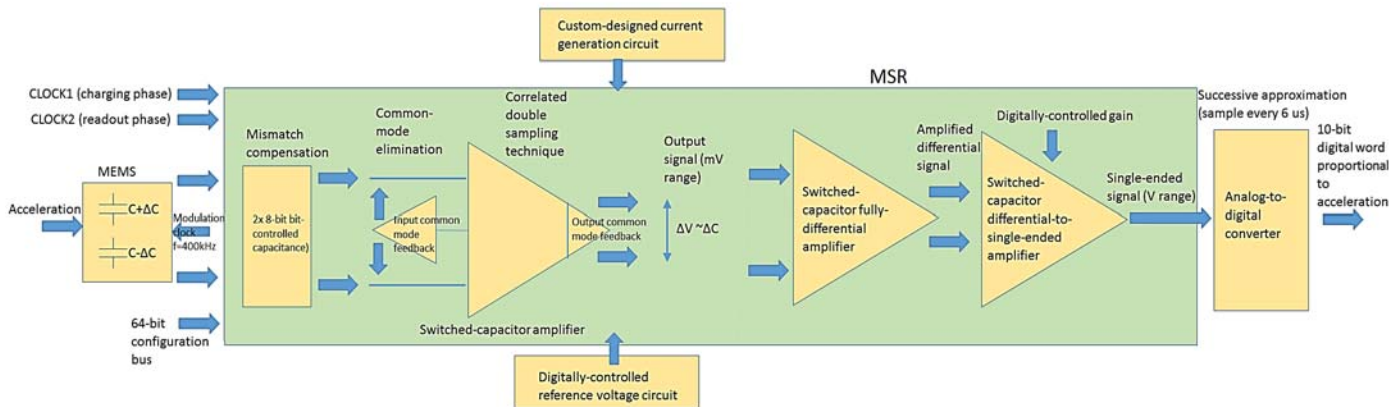


Fig. 7. Block diagram of the MSR module.

Since the ASIC and MEMS are designed as separate chips, direct bonding of both chips in one package will be required. Consequently, the pads of the both chips should be placed on opposite sides of each chip to allow straightforward bonding. Moreover, in the ASIC additional blocks called MEMS Mocks (MM) were also designed in order to emulate MEMS capacitances. The values of MM capacitances are digitally controlled and enable the verification of the ASIC functionality before it is bonded with MEMS.

We performed simulations of MSR schematic with sinusoidal input acceleration (from $-2g$ to $+2g$) with the frequency of 10 kHz. Fig. 8 and Fig. 9 show the obtained results after particular MSR stages. After the first stage, a small differential voltage signal proportional to the capacitance

change is obtained (Fig. 8, top). Note that due to the switched-capacitor nature of the circuit, the signal is only valid in particular time instants, hence the noise visible in the signal due to switching do not really have influence on the final results. Next, this signal has to be amplified in the second stage, a constant gain of 20 for this amplifier was chosen. It can be seen in Fig. 8 that the amplitude of the sinusoidal signal after the second stage is almost exactly 20 times higher than the amplitude of the signal after the first stage. The third stage amplifies the signal further (the gain here is digitally controlled, for this simulation we chose a gain of 16) and additionally converts it from differential to single-ended form. It can be observed that after sampling at the output of the third stage, the signal does no longer contain glitches.

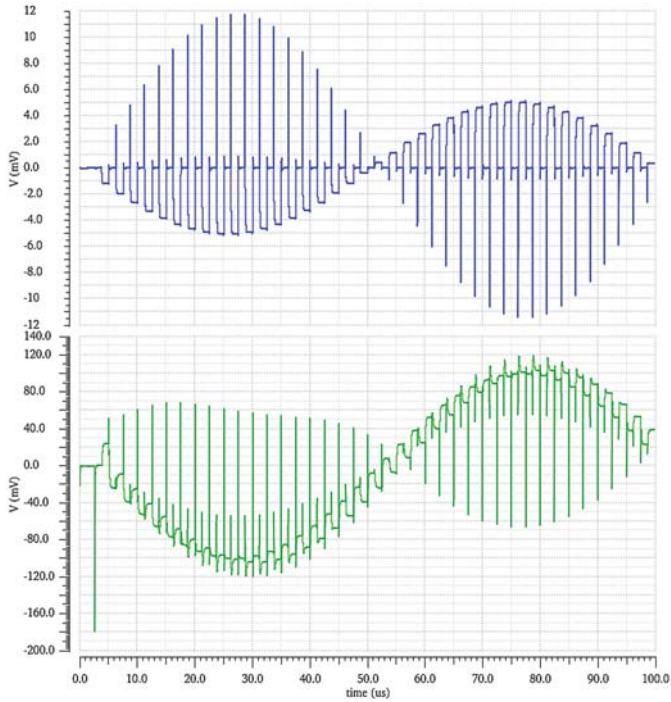


Fig. 8. Output signal of the first MSR stage (top) and second stage (bottom).

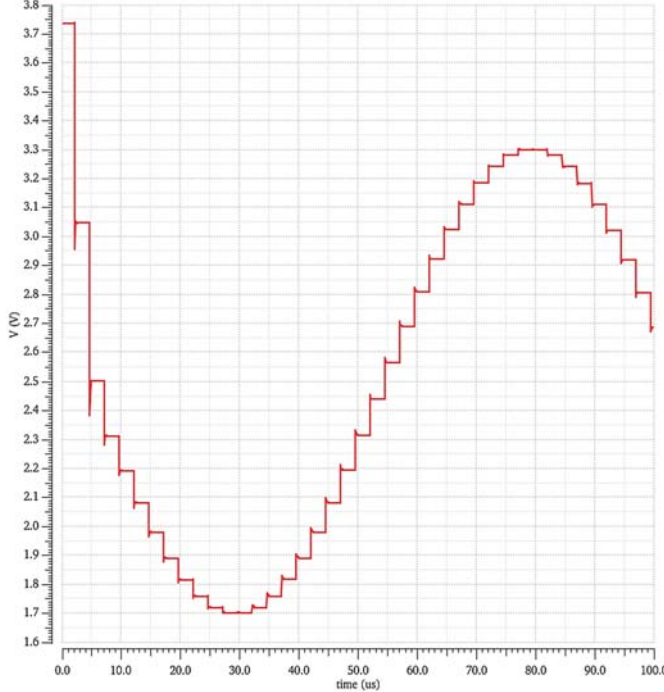


Fig. 9. Sampled output signal of the MSR.

C. Floorplan

Fig. 10. shows the floorplan of the ASIC. The estimated size of the chip is $2.5 \text{ mm} \times 2.5 \text{ mm}$. Pads are arranged symmetrically. MEMS I/O pads are placed on the left side in order to bond them directly with output pads of the MEMS. This is necessary in order to ensure the best signal quality between chips (low resistance connections, minimizing parasitic capacitances and inductances, etc.). The positions of the pads affect placement of main blocks.

The mixed design technique is used to prepare the floorplan [12]. Top-down technique is used to place the main blocks of the ASIC top-level, and the main blocks are designed using bottom-up technique.

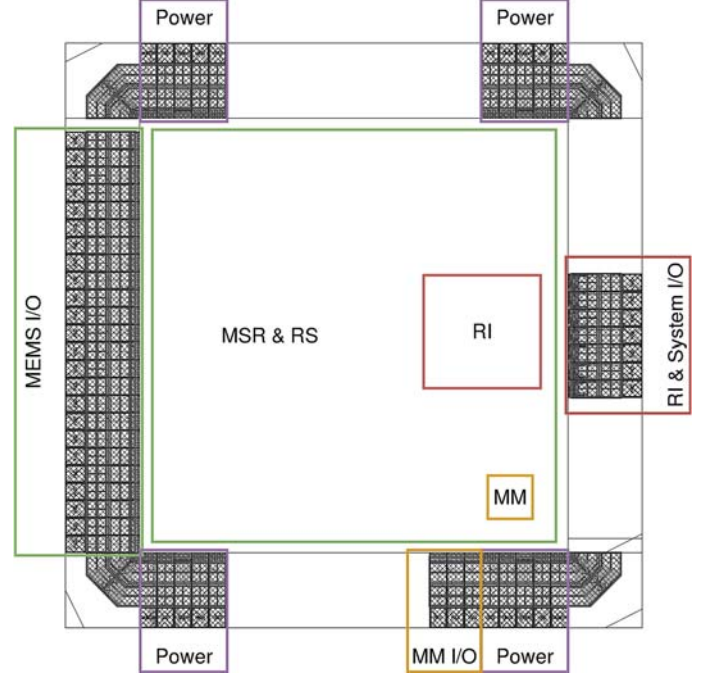


Fig. 10. ASIC floorplan view.

IV. CONCLUSIONS

In the paper one-axis accelerometers were first analysed. Based on this analysis, two structures were designed and tested. The simulations have shown that the designed MEMS sensors correctly convert the acceleration into capacitance. Although their sensitivity is quite low, it is sufficient to measure the acceleration characteristic for human movement. Moreover, based on the results obtained from MEMS accelerometer simulation, a readout circuit was designed. Its simulations showed that it can be successfully used to convert a small change in MEMS capacitance to the voltage necessary for the ADC. Therefore, we can conclude, that the dual System-on-Chip (MEMS as inertial sensor and ASIC as readout circuit) can fulfil the project requirements, i.e., its parameters allow it to be used in a system for the diagnosis of human imbalance disorders.

REFERENCES

- [1] Aaltonen L, "Integrated interface electronics for capacitive MEMS inertial sensors", PhD dissertation, 2010
- [2] Abbasi-Kesbi R, Nikfarjam A, "Denoising MEMS accelerometer sensors based on L2-norm total variation algorithm", Electronics Letters, Vol. 53, No. 5, pp. 322-324, 2017
- [3] Ahsan Shahzad, Seunguk Ko, Samgyu Lee, Jeong-A Lee, Kiseon Kim, "Quantitative Assessment of Balance Impairment for Fall-Risk Estimation Using Wearable Triaxial Accelerometer", IEEE Sensors Journal, Vol. 17, No. 20, pp. 6743-6751, 2017
- [4] Allen P.E, Holberg D.R, "CMOS Analog Circuit Design", Oxford University Press, 2002

- [5] Amini B.V, Ayazi F, "A 2.5-V 14-bit $\Sigma\Delta$ CMOS SOI capacitive accelerometer", in IEEE Journal of Solid-State Circuits, vol. 39, no. 12, pp. 2467-2476, Dec. 2004
- [6] Ankita Jain, Vivek Kanhangad, "Human Activity Classification in Smartphones Using Accelerometer and Gyroscope Sensors", IEEE Sensors Journal, Vol. 18, No. 3, pp. 1169-1177, 2018
- [7] Azza Allouch; Anis Koubâa; Tarek Abbes; Adel Ammar, "RoadSense: Smartphone Application to Estimate Road Conditions Using Accelerometer and Gyroscope", IEEE Sensors Journal, Vol. 17, No. 13, pp. 4231-4238, 2017
- [8] Baker R.J, "CMOS Circuit Design, Layout and Simulation", Wiley, 2010
- [9] Bluetooth, IEEE Standard 802.15
- [10] Bryzek J, Roundy S, Bircumshaw B, Chung C, Castellino K, Stetter R, Vestel M, "Marvelous MEMS", IEEE Circuits and Devices Magazine, Vol. 22, No. 2, pp. 8-28, 2006
- [11] Cadence Custom IC Design, <https://www.cadence.com/>
- [12] Chen J., Henrie M., Mar M. F., Nizic M., Mixed-Signal Methodology Guide, 2012
- [13] Coventor MEMS Solution and Design, <https://www.coventor.com/>
- [14] Fang D, "Low-noise and Low-power Interface Circuits Design for Integrated CMOS-MEMS Inertial Sensors", PhD dissertation, 2006
- [15] Fullerton E, Heller B, Munoz-Organero M, "Recognizing Human Activity in Free-Living Using Multiple Body-Worn Accelerometers", IEEE Sensors Journal, Vol. 17, No. 16, pp. 5290-5297, 2017
- [16] Gad el Hak M, "The MEMS Handbook", CRC Press, USA, 2002
- [17] Hao Kang, Jing Yang, Honglong Chang, "A Closed-Loop Accelerometer Based on Three Degree-of-Freedom Weakly Coupled Resonator With Self-Elimination of Feedthrough Signal", IEEE Sensors Journal, Vol. 18, No. 10, pp. 3960-3967, 2018
- [18] Honglin Xu, Junjie Wu, Hao Zhang, Haitao Liu, Qing Deng, "A 10 mW, 0.4 $\mu\text{g}/\sqrt{\text{Hz}}$, 700 Hz Sigma-Delta High-Order Electromechanical Modulator for High-Q Micromechanical Capacitive Accelerometer", IEEE Sensors Journal, Vol. 18, No. 3, pp. 1187-1194, 2018
- [19] Jaehoon Jun, Cyuyeol Rhee, Sangwoo Kim, Suwan Kim, "An SC Interface With Programmable-Gain Embedded $\Delta\Sigma$ ADC for Monolithic Three-Axis 3-D Stacked Capacitive MEMS Accelerometer", IEEE Sensors Journal, Vol. 17, No. 17, pp 5558-5568, 2017
- [20] Jing Yang, Jiming Zhong, Honglong Chang, "A Closed-Loop Model-Localized Accelerometer", Journal of Microelectromechanical Systems, Vol. 27, No. 2, pp. 210-217, 2018
- [21] Kamarainen M, "Low-power Front-ends for Capacitive Three-axis Accelerometers", PhD dissertation, 2010
- [22] Kazama A, Aono T, Okada R, "High Shock-Resistant Design for Wafer-Level-Packaged Three-Axis Accelerometer With Ring-Shaped Beam", Journal of Microelectromechanical Systems, Vol. 27, No. 2, pp. 355-364, 2018
- [23] Kepski M, Kwolek B, "Event-driven system for fall detection using body-worn accelerometer and depth sensor", IET Computer Vision, Vol. 12, No. 1, pp. 48-58, 2018
- [24] Kosobutskyy P, Komarnutskyy M, Maj C, Zajac P, Szermer M, Zabierowski W, "Monte Carlo Modeling of Stiffness of MEMS Membrane", in Proc. International Conference MIXDES, Lublin, Poland, pp. 97-100, June 19-21, 2014
- [25] Kuo J.B, Lin S-H, "Low-Voltage SOI CMOS VLSI Devices and Circuits", Wiley, 2001
- [26] Kyberd P.J, Poulton A, "Use of Accelerometers in the Control of Practical Prosthetic Arms", IEEE Transactions on Neural Systems and Rehabilitation Engineering, Vol. 25, No. 10, pp. 1884-1891, 2017
- [27] Lahdenoja O, Hurnanen T, Iftikhar Z, Nieminen S, Knuutila T, Saraste A, Kiviniemi T, Vasankari T, Airaksinen J, Päkkälä M, Koivisto T, "Atrial Fibrillation Detection via Accelerometer and Gyroscope of a Smartphone", IEEE Journal of Biomedical and Health Informatics, Vol. 22, No. 1, pp. 108-118, 2018
- [28] Lemkin M, Boser B.E, "A three-axis micromachined accelerometer with a CMOS position-sense interface and digital offset-trim electronics", in IEEE Journal of Solid-State Circuits, vol. 34, no. 4, pp. 456-468, Apr 1999
- [29] Lin Ye, Ying Guo, Steven W. Su, "An Efficient Autocalibration Method for Triaxial Accelerometer", IEEE Transactions on Instrumentation and Measurement, Vol. 66, No. 9, pp. 2380-2390, 2017
- [30] Maj C, Szermer M, Napieralski A, Kirjusha B, Tchkalov A, Michalik P, "Macro Model of Capacitive MEMS Accelerometer in Cadence Environment", in Proc. International Conference on Thermal, Mechanical and Multi-Physics Simulation and Experiments in Microelectronics and Microsystems, EuroSimE, Montpellier, France, pp. 1-5, April 17-20, 2016
- [31] Maluf N, "An Introduction to Micromechanical Systems Engineering", Artech House, USA, 2000
- [32] Melnyk M, Kurnytskyy A, Lobur M, Zajac P, Szermer M, Maj C, Zabierowski W, "Optimization of Microelectric Actuator Design Using Golden Section Search to Get the Defined Output Characteristics", Visnik 808, s. 77-84, 2014
- [33] Meng Zhao, Zhongjian Chen, Wengao Lu, Yacong Zhang, Yuze Niu, Guangyi Chen, "A High-Voltage Closed-Loop SC Interface for a ± 50 g Capacitive Micro-Accelerometer With 112.4 dB Dynamic Range", IEEE Transactions on Circuits and Systems I: Regular Papers, Vol. 64, No. 6, pp. 1328-1341, 2017
- [34] Motorola, Serial Peripheral Interface Bus
- [35] Napieralski A, Maj C, Szermer M, Zajac P, Zabierowski W, Napieralska M, Starzak L, Zubert M, Kielbik R, Amrozik P, Ciota Z, Ritter R, Kaminski M, Kotas R, Marciniak P, Sakowicz B, Grabowski K, Sankowski W, Jablonski G, Makowski D, Mielczarek A, Orlikowski M, Jankowski M, Perek P, "Recent Research in VLSI, MEMS and Power Devices with Practical Application to the ITER and DREAM Projects", Facta Universitatis, Electronics and Energetics Series, Vol. 27, No. 4, pp. 561-588, December 2014
- [36] Napieralski A, Napieralska M, Szermer M, Maj C, "The evolution of MEMS and modelling methodologies", COMPEL: The International Journal for Computation and Mathematics in Electrical and Electronic Engineering, Vol. 31, No. 5, pp. 1458-1469, 2012
- [37] Nazdrowicz J, "SIMULINK and COMSOL Software Application for MEMS Accelerometer Modeling and Simulation", in Proc. International Conference MIXDES, Bydgoszcz, Poland, pp. 429-434, June 22-24, 2017
- [38] Nazdrowicz J, Napieralski A, "Electrical Equivalent Model of MEMS Accelerometer in Matlab/SIMULINK Environment", in Proc. International Conference MEMSTECH, Polyana, Ukraine, pp. 69-72, April 18-22, 2018
- [39] Nazdrowicz J, Szermer M, Maj C, Napieralski A, "Different Methods of Capacitive Comb Drive MEMS Accelerometer Simulations", in Proc. Baltic URSI Symposium 2018, Poznań, Poland, pp. 1027-1029, May 14-17, 2018
- [40] Nevlyudov I, Yevsieiev V, Bortnikova V, Miliutina S, "MEMS accelerometers production technological route selection", in Proc. International Conference CADSM, Polyana, Ukraine, pp. 424-427, February 21-25, 2017
- [41] Nevlyudov I, Yevsieiev V, Miliutina S, Bortnikova V, "Accelerometers production technological process decomposition parameters model", in Proc. International Conference MEMSTECH, Polyana, Ukraine, pp. 1-5, April 20-24, 2016
- [42] Nevlyudov I, Ponomaryova G, Miliutina S, Bortnikova V, "MEMS accelerometers classification using machine-learning methods", in Proc. International Conference MEMSTECH, Polyana, Ukraine, pp. 51-55, April 20-23, 2017
- [43] Olli Särkkä; Tuukka Nieminen; Saku Suuriniemi; Lauri Kettunen, "A Multi-Position Calibration Method for Consumer-Grade Accelerometers, Gyroscopes, and Magnetometers to Field Conditions", IEEE Sensors Journal, Vol. 17, No. 11, pp. 3470-3481, 2017
- [44] Ozel M.K, Cheperak M, Dar, Kiaei S, Bakkaloglu B, Ozev S, "An Electrical-Stimulus-Only BIST IC for Capacitive MEMS Accelerometer Sensitivity Characterization", IEEE Sensors Journal, Vol. 17, No. 3, pp. 695-708, 2017
- [45] Pengyu Gao, Kui Li, Tianxiao Song, Zengjun Liu, "An Accelerometers-Size-Effect Self-Calibration Method for Triaxis Rotational Inertial Navigation System", IEEE Transactions on Industrial Electronics, Vol. 65, No. 2, pp. 1655-1664, 2018
- [46] Pratool Bharti, Anurag Panwar, Ganesh Gopalakrishna, Sriram Chellappan, "Watch-Dog: Detecting Self-Harming Activities From Wrist Wear Accelerometers", IEEE Journal of Biomedical and Health Informatics, Vol. 22, No. 3, pp. 686-696, 2018
- [47] Ranjbaran S, Ebadiollahi S, "Fast and precise solving of non-linear optimisation problem for field calibration of triaxial accelerometer", Electronics Letters, Vol. 54, No. 3, pp. 148-150, 2018

- [48] Razavi B, "Design of Analog CMOS Integrated Circuits", McGraw Hill, 2001
- [49] Rödjemård H, Lööf A, "A differential charge-transfer readout circuit for multiple output capacitive sensors", In Sensors and Actuators A: Physical, Volume 119, Issue 2, 2005, pp. 309-315
- [50] Sun H, "Sensing and Control Electronics Design for Capacitive CMOS-MEMS Inertial Sensors", PhD dissertation, 2011
- [51] Szermer M, Nazdrowicz J, Zabierowski W, "FEM Analysis of a 3D Model of a Capacitive Surface-micromachined Accelerometer", in Proc. International Conference CADSM, Polyana, Ukraine, pp. 432-434, February 21-25, 2017
- [52] Szermer M, Zajac P, Starzak L, "Influence of geometry scaling on comb-drive accelerometer performance", in Proc. International Conference MEMSTECH, Polyana, Ukraine, pp. 118-121, April 18-22, 2018
- [53] Tse C, "Design of a Power Scalable Capacitive MEMS Accelerometer Front End", PhD dissertation, 2013
- [54] Uyemura J.P., "CMOS Logic Circuit Design", Kluwer Academic Publishers, 2001
- [55] Wu J, "Sensing and Control Electronics for Low-Mass Low-Capacitance MEMS Accelerometers", PhD dissertation, 2002
- [56] Xiangge He, Min Zhang, Shangran Xie, Fei Liu, Lijuan Gu, Duo Yi, "Self-Referenced Accelerometer Array Multiplexed on a Single Fiber Using a Dual-Pulse Heterodyne Phase-Sensitive OTDR", Journal of Lightwave Technology, Vol. 36, No. 14, pp. 2973-2979, 2018
- [57] Xiaofeng Wang, Yongxing Guo, Li Xiong, Heng Wu, "High-Frequency Optical Fiber Bragg Grating Accelerometer", IEEE Sensors Journal, Vol. 18, No. 12, pp. 4954-4960, 2018
- [58] Yu-Te Liao, Shih-Chieh Huang, Fu-Yuan Cheng, Tsung-Heng Tsai, "A Fully-Integrated Wireless Bondwire Accelerometer With Closed-loop Readout Architecture", IEEE Transactions on Circuits and Systems I: Regular Papers, Vol. 62, No. 10, pp. 2445-2453, 2015
- [59] Zakriya Mohammed, Waqas A. Gill, Mahmoud Rasras, "Double-Comb-Finger Design to Eliminate Cross-Axis Sensitivity in a Dual-Axis Accelerometer", IEEE Sensors Letters, Vol. 1, No. 5, 2017
- [60] Zega V, Credi C, Bernasconi R, Langfelder G, Magagnin L, Levi M, Corigliano A, "The First 3-D-Printed z-Axis Accelerometers With Differential Capacitive Sensing", IEEE Sensors Journal, Vol. 18, No. 1, pp. 53-60, 2018



Michał Szermer was born in Łódź, Poland, in 1973. He received the MSc and PhD degrees from Łódź University of Technology (TUL), Poland, in 1998 and 2004, respectively. His research focuses on the integrated circuits design with special consideration of mixed-signal circuits. He took part in many projects related to ASIC modelling and design. He is also involved in modelling, design and analysis of MEMS. Recently, he is designing of MEMS inertial sensors for the medical systems and applications.



Piotr Amrozik received MSc (2006) and PhD degrees (2012) in electronics from Łódź University of Technology. His research focuses on design methodologies, EDA tools and architectures of integrated circuits and FPGAs. He took part in several international and national research projects and coordinated two national research projects (2010-2013). He is an author and co-author of three issued patents and several scientific publications in international journals and conference proceedings.



Piotr Zająć received his diploma in electronics from the Faculty of Electrical, Electronic, Computer and Control Engineering, Łódź University of Technology, Poland (2005) and his PhD from the Department of Electrical and Computer Engineering, National Institute of Applied Sciences of Toulouse, France (2008). He is an Assistant Professor at the Department of Microelectronics and Computer Science at the Technical University of Łódź. His research interests include processor architecture and design, fault tolerance in multi-core systems and thermal challenges in modern ICs. He has published more than 60 papers in peer reviewed transactions, journals and conference proceedings.



Cezary Maj was born in Łódź, Poland, in 1982. He received the MSc degree in electronics from Łódź University of Technology (TUL), Poland, in 2005 and PhD degree in microelectronics from both TUL and Institut National des Sciences Appliquées de Toulouse (INSA), France. He specializes in microelectronics and his research focuses on modelling, fabrication and characterization of microsystems. He took part in a few projects connected with development of sensors for various applications. Recently, he is involved in MEMS modelling and investigation of thermal problems in current multicore processors.



Andrzej Napieralski received the MSc and PhD degrees from the Łódź University of Technology (TUL), Poland in 1973 and 1977, respectively, and a DSc degree in Electronics from the Warsaw University of Technology (WUT), Poland and in Microelectronics from the Université de Paul Sabatier (UPS), France in 1989. Since 1996 he has been Director of the Department of Microelectronics and Computer Science. Between 2002 and 2008 he was Vice-President of TUL. He is an author or co-author of over 960 publications and editor of 19 conference proceedings and 12 scientific journals. He has supervised 45 PhD theses; six of them received the Prime Minister of Poland prize. In 2008 he received the Degree of Honorary Doctor of Yaroslav the Wise Novgorod State University, Russia.